Remote Sensing of Environment 113 (2009) 1443–1452

Contents lists available at ScienceDirect

Remote Sensing of Environment

journal homepage: www.elsevier.com/locate/rse

Integration of MODIS-derived metrics to assess interannual variability in snowpack, lake ice, and NDVI in southwest Alaska

Bradley Reed [a,*], Michael Budde [b], Page Spencer [c], Amy E. Miller [c]

[a] U.S. Geological Survey (USGS), Reston, VA 20191, United States
[b] USGS Center for Earth Resources Observation and Science (EROS), Sioux Falls, SD 57198, United States
[c] National Park Service, Anchorage, AK 99501, United States

ARTICLE INFO

Article history:
Received 30 November 2007
Received in revised form 7 July 2008
Accepted 31 July 2008

Keywords:
Moderate Resolution Imaging Spectroradiometer (MODIS)
Snow cover
Lake ice
Normalized difference vegetation index (NDVI)
Phenology
Ecosystem monitoring

ABSTRACT

Impacts of global climate change are expected to result in greater variation in the seasonality of snowpack, lake ice, and vegetation dynamics in southwest Alaska. All have wide-reaching physical and biological ecosystem effects in the region. We used Moderate Resolution Imaging Spectroradiometer (MODIS) calibrated radiance, snow cover extent, and vegetation index products for interpreting interannual variation in the duration and extent of snowpack, lake ice, and vegetation dynamics for southwest Alaska. The approach integrates multiple seasonal metrics across large ecological regions.

Throughout the observation period (2001–2007), snow cover duration was stable within ecoregions, with variable start and end dates. The start of the lake ice season lagged the snow season by 2 to 3 months. Within a given lake, freeze-up dates varied in timing and duration, while break-up dates were more consistent. Vegetation phenology varied less than snow and ice metrics, with start-of-season dates comparatively consistent across years. The start of growing season and snow melt were related to one another as they are both temperature dependent. Higher than average temperatures during the El Niño winter of 2002–2003 were expressed in anomalous ice and snow season patterns. We are developing a consistent, MODIS-based dataset that will be used to monitor temporal trends of each of these seasonal metrics and to map areas of change for the study area.

Published by Elsevier Inc.

1. Introduction

Ecosystem responses to changing climate are expected to occur over different temporal scales, with the timing of seasonal events (e.g., freeze–thaw cycles, snowpack formation and snowmelt, and the onset or end of the growing season) showing a great deal of variability. Long-term changes in snowpack, lake ice, and vegetation may be particularly pronounced in high northern latitudes where small changes in climate can alter the timing of these events. Remotely sensed data can potentially capture much of this variation in seasonality, and provided that the data record is sufficiently long, enable us to distinguish between interannual variability and multi-year trends (e.g., in snowpack duration or growing season length).

Here, we describe the use of Moderate Resolution Imaging Spectroradiometer (MODIS) data from Aqua and Terra satellites to monitor snow cover, lake ice, and vegetation dynamics in a network of national parks and wildlife refuges in southwest Alaska. The moderate spatial resolution (250–1000 m) and high temporal resolution (1–16 days) provided by MODIS enables frequent observations of a region characterized by a rapidly changing landscape, complex climatic regime, frequent cloud cover, and little infrastructure to support ground-based measurements. Standard MODIS data products were used to derive ecosystem metrics, including extent and duration of snow cover (500 m, 8-day snow cover extent), the timing of ice formation and break-up on large lakes (250 m daily calibrated radiance and corresponding browse images), and variation in vegetation growing season (250 m, 16-day Vegetation Index) across the region. This paper describes our efforts to develop a set of derived metrics from MODIS products for long-term monitoring of seasonal events, and to integrate these metrics to better understand the spatial variability and temporal dynamics of the ecosystems of southwest Alaska.

1.1. Background

Increasing temperatures projected for the northern high latitudes over the next century are expected to influence a number of seasonal events including snowpack formation, lake ice formation and break-up, and onset of growing season. Milder winters have resulted in later freeze-up dates, earlier break-up dates, or both for lakes in the northern United States and Canada (Magnuson et al., 2000) and are expected to affect the frequency and severity of ice dams, floods, and low flows in the Arctic. Reduced snow cover and/or snow depth and

* Corresponding author. Tel.: +1 703 648 5536; fax: +1 703 648 5542.
E-mail address: reed@usgs.gov (B. Reed).

0034-4257/$ – see front matter. Published by Elsevier Inc.
doi:10.1016/j.rse.2008.07.020

earlier snowmelt dates have also been observed at high latitudes (Lammers et al., 2001; Zhang et al., 2001), and these changes in snow cover have been found to alter the timing of river discharge (Déry et al., 2005). Earlier snowmelt dates also lengthen the growing season by enabling plant growth to start earlier (Hicke et al., 2002; Delbart et al., 2005). Earlier start-of-season dates, in turn, are thought to have led to increases in indices of vegetation greenness (e.g., normalized difference vegetation index (NDVI)) and biomass in recent decades over large regions of Alaska, northwestern Canada, and northern Eurasia (Myneni et al., 1997, 2001; Goetz et al., 2005; Reed, 2006).

In southwest Alaska, the seasonality of snowpack, lake ice, and vegetation dynamics are expected to have wide-reaching effects. The climate is influenced by complex interactions of several forcing agents, all functioning at different temporal scales: the El Niño and La Niña Southern Oscillation (one–two years), the Pacific Decadal Oscillation (20–30 years) and the Pacific/North American circulation pattern (days to weeks), as well as local forcings resulting from topography (Papineau, 2001). These climatic factors influence the depth, timing, and spatial extent of snowpack that, subsequently, affect soil thermal regimes and the timing of freeze–thaw events, lake ice thickness, and surface and groundwater hydrology in the region. Vegetation dynamics (e.g., Sturm et al., 2005) and wildlife foraging, movement, and predation (e.g., Adams et al., 1995; Modafferi & Becker, 1997) are also affected by snowpack. An increase in growing season length, as observed in the Bristol Bay Lowlands and Kuskowim Delta of southwest Alaska (Reed, 2006), is expected to result in increases in plant biomass that can lead to changes in community composition. Such climate-driven effects on habitat and forage may affect wildlife populations, including caribou, moose, wolves, and a number of other predator and prey species. The presence or absence of lake ice and snow also affects winter access to subsistence activities by rural residents who depend on these resources (e.g., ice fishing, hunting, trapping, firewood collection) (Gaul, 2007).

Accurate measurements of regional-scale vegetation, snowpack and lake ice dynamics are needed to improve our understanding of the long-term effects of climate on southwest Alaska ecosystems. The National Park Service's Inventory and Monitoring (I&M) Program has begun to monitor these variables as a means of characterizing short- and long-term variation in seasonality. Remote sensing data can provide the synoptic coverage and temporal resolution necessary for monitoring trends in snowpack, lake ice, and vegetation dynamics in this otherwise remote and inaccessible, region. Moderate resolution remote sensing provides a means for quantifying land surface characteristics such as land cover type and extent, snow cover extent, surface temperature, leaf area index, and fire occurrence. High quality, consistent, and well-calibrated satellite measurements are needed if we are to monitor trends in these seasonal variables. The high temporal resolution of MODIS data makes them especially well-suited to capture variation in the timing of seasonal events across years.

2. Methods

2.1. Study area

The study area (Fig. 1) comprises nearly 20 million ha of land between about 56–62° N latitude and 148–160° W longitude in southwest Alaska. It includes the Southwest Alaska Network (SWAN), one of 32 networks in the U.S. National Park Service's (NPS) Inventory and Monitoring Program (Fancy et al., 2009), which consists of five National Park Service units (Alagnak Wild River, Aniakchak National Monument & Preserve, Katmai National Park & Preserve, Kenai Fjords National Park, Lake Clark National Park & Preserve). Also included are five National Wildlife Refuges (NWR) (Kenai NWR, Becharof NWR, Alaska Peninsula NWR, Kodiak NWR, and portions of Alaska Maritime NWR). Together, these parks and refuges total more than 6.2 million ha of protected land area. This study was initiated as part of the NPS Vital Signs monitoring effort.

For this paper we selected three focus areas that span boreal, maritime, and transitional climatic regimes in southwest Alaska (Simpson et al., 2007). The selection of these areas ensured a spatial coherence among metrics and minimized variation due to climate, topography (elevation), vegetation, and permanent snow and ice. Five large lakes contained within the focus areas were used to represent lake ice dynamics (freeze-up and break-up) across a range of ecoregions (Table 1).

The focus areas were derived from the intersection of ecoregion (Nowacki et al., 2002) and National Park and National Wildlife Refuge boundaries: Cook Inlet Basin ecoregion and Kenai National Wildlife Refuge (transition), Lime Hills ecoregion and Lake Clark National Park & Preserve (boreal), and Alaska Peninsula ecoregion and Katmai National Park & Preserve (maritime) (Fig. 1). Ecoregions are large ecosystems (millions of hectares) that are primarily defined by climate and topography, with local refinements from vegetation, lithology, and surficial geomorphology.

The focus areas are characterized by diverse terrain, ranging from gently rolling coastal lowlands to steep, dissected mountain ranges and glaciated valleys. Elevation ranges from 0 to 3100 m. Mean annual precipitation ranges from 400–600 mm in the western interior (Lime Hills and Alaska Peninsula), to 3000–4000 mm at higher elevations and along the eastern coastline of the Cook Inlet Basin (Davey et al., 2007). Mean annual temperature ranges from −8 °C in the western interior to 4 °C in the coastal lowlands, with the growing season generally limited to May–October at lower elevations. Winter temperatures at lower elevations in the region fluctuate around 0 °C. Vegetation in the study area reflects the climatic patterns and is composed primarily of coniferous forests and shrublands along the northern coasts, mixed hardwood-coniferous forests and grasslands at mid-elevations in the interior, and wetlands, tundra, and dwarf shrub communities at higher elevations. Receding glaciers and repeated volcanic activity have resulted in large areas of exposed substrate that are being rapidly colonized by vegetation.

2.2. MODIS data

The MODIS sensors aboard the Terra and Aqua satellites are part of the National Aeronautics and Space Administration's (NASA's) Earth Observing System (EOS). The MODIS sensors acquire data in 36 spectral bands and at three spatial resolutions ranging from 250 to 1000 m (Justice et al., 1997). The Terra and Aqua satellites were launched in 1999 and 2002, respectively, and MODIS data have been collected continuously since February 2000. A swath width of 2330 km enables near-global coverage every day, with multiple swaths collected daily over southwest Alaska. The calibration, spatial detail, and spectral and geolocation quality of MODIS data improved on its predecessor, the Advanced Very High Resolution Radiometer (AVHRR), which provided 4- to 6-band multispectral data at a resolution of 1.1 km (Townshend & Justice, 2002). A large number of standard, regularly generated products from MODIS are designed for land, ocean, and atmospheric science applications. This research uses a limited set of Terra MODIS land products: snow cover extent, calibrated radiance (for lake ice), and vegetation index (Justice et al., 1997).

2.2.1. Snow extent

The MODIS snow cover mapping algorithm uses satellite reflectance data collected in MODIS bands 4 (0.545–0.565 μm) and 6 (1.628–1.652 μm) to calculate the normalized difference snow index (NDSI; Eq. (1)) (Hall et al., 1995).

$$\mathrm{NDSI} = (\text{band } 4 - \text{band } 6) / (\text{band } 4 + \text{band } 6) \tag{1}$$

The process uses the NDSI value and band 2 (0.841–0.876 μm) reflectance criteria, along with numerous threshold tests, to define a pixel as snow. Daily measures of snow cover extent at 500-meter

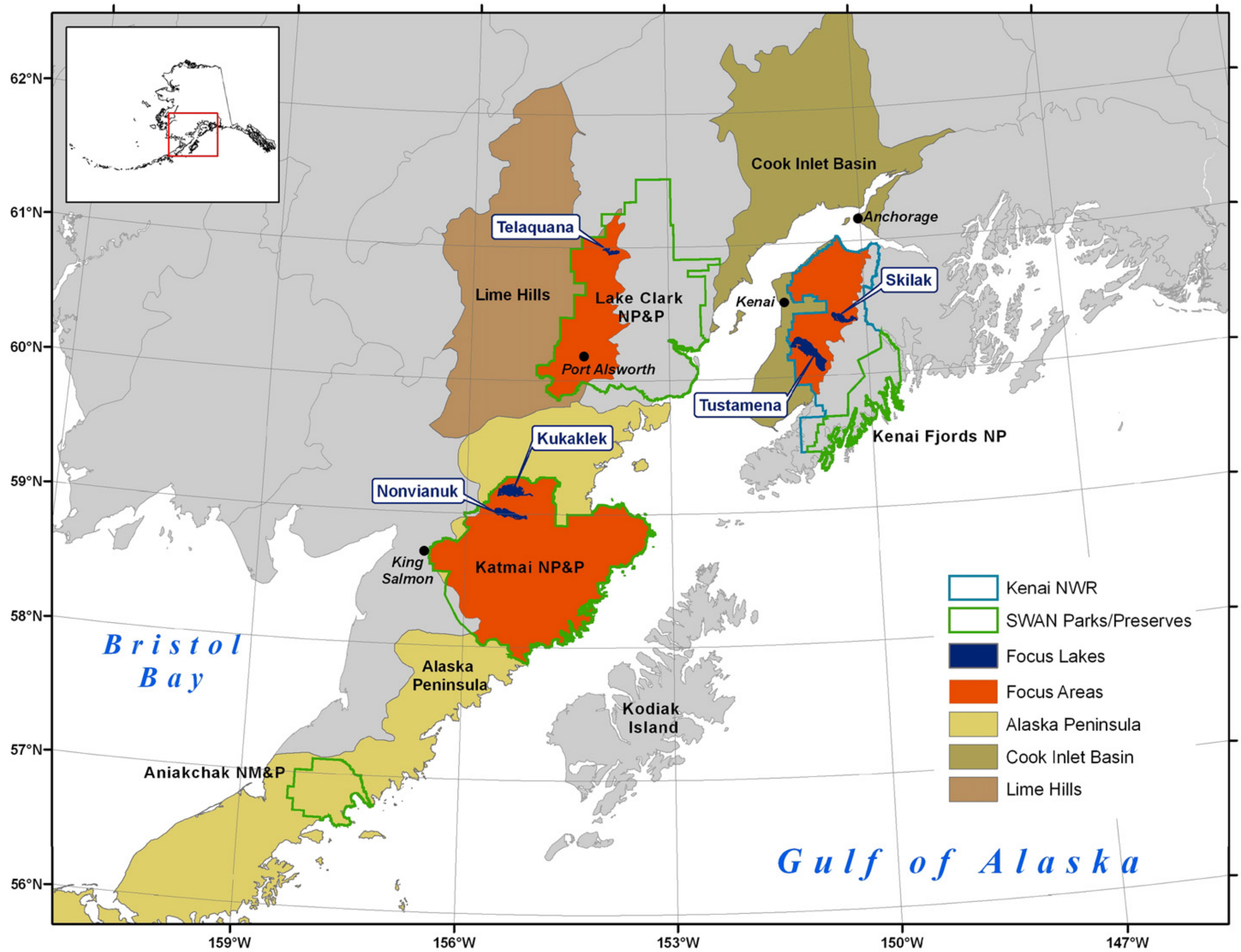

Fig. 1. The study area in southwest Alaska with ecoregions, park boundaries, and highlighted focus areas.

resolution (highest resolution available for this product) are created and further combined into 8-day composites to help minimize cloud effects. The snow mapping algorithm classifies pixels as snow, snow-covered lake ice, cloud, water, land or other. Assessments of these products show overall accuracies of ~93%, with variability due to land cover type and snow condition (Hall & Riggs, 2007).

We used areal snow cover depletion curves for deriving important timing metrics that could be applied to an assessment of interannual snow cover variability. The application of snow curves derived timing and duration metrics for the selected focus areas. The primary metrics of interest included the timing of snow cover onset, the timing of seasonal snowmelt, and the duration of the snow season.

We created seasonal snow cover accumulation and depletion curves by calculating the percentage of snow-covered area within each focus area for every 8-day MODIS period. The timing of metrics for the start and end of the snow season were determined by applying thresholds to the time series of percentage estimates and selecting the 8-day period that first exceeded the threshold at the start of the season and the first period to fall below the threshold at the end of the season. To eliminate false start and end of seasons due to early-season snowfalls or short-term spring melting events, we required that the threshold be maintained for a minimum of two periods beyond the flagged date. The duration of the snow season was the number of days between the start and end of the snow season.

The thresholds for defining the start and end of the snow season were determined through visual interpretation of the percent snow cover graphs and consideration of seasonal snow and ice cover characteristics for each of the focus areas. At the beginning of the snow season, major snow cover accumulations occurred shortly after the 20% cover threshold was reached. Likewise, at the end of the snow season, there were often rapid depletions in snow covered area and very few snow events after percentages fell below 20%. The Cook Inlet Basin and the Lime Hills areas were similar in that they exhibited little permanent snow and ice cover throughout the non-snow season. We

Table 1
Focus areas for vegetation, snow, and lake ice metrics.

Lake	Ecoregion	Protected area	Size (ha)	Lake Elevation (m)
Skilak	Cook Inlet Basin	Kenai National Wildlife Refuge	9900	60
Tustemena	Cook Inlet Basin	Kenai National Wildlife Refuge	29,700	60
Telaquana	Lime Hills	Lake Clark National Park & Preserve	4700	365
Kukaklek	Alaska Peninsula	Katmai National Park & Preserve	17,300	300
Nonvianuk	Alaska Peninsula	Katmai National Park & Preserve	13,200	180

therefore applied the threshold of 20% for these areas. The Alaska Peninsula retained 5–10% snow and ice cover throughout the year, so we used the upper limit of that range and applied a threshold of 30% for this area.

An additional consideration in determining snow cover metrics is the impact of clouds on percent area calculations. The MODIS snow cover product contains a classified cloud value which was used to identify cloudy pixels in each 8-day composite image. In addition to verifying that the data passed initial science quality flags, as provided in the product metadata, we evaluated the quality of the snow cover extent data by visually comparing measurements with MODIS surface reflectance data. We calculated percent areas for cloud cover and compared the occurrence of high cloud percentages with reductions in snow cover percent. There was a direct correspondence between dramatic reductions in snow-covered area for a single composite period and the presence of clouds. Dramatic declines in the percent snow covered area could be attributed to high percentage of clouds in nearly every case, meaning that those pixels were likely to be snow covered in the absence of clouds. We use these comparisons to more accurately apply the thresholds described above.

2.2.2. Lake ice

We made extensive use of the browse images provided by the MODIS Rapid Response System (Rapidfire images), which are created in near-real time for all MODIS granules (http://rapidfire.sci.gsfc.nasa.gov/). The natural-color composites (which use only visible wavelengths) of the images were used for the lake ice cover interpretations. The Rapidfire images were more quickly accessible (near-real time), required no additional processing, and were more consistent than processed reflectance or radiance data. We compared interpretations of lake ice cover using Rapidfire images and enhanced composites of the Level 1B (L1B) calibrated radiance images. L1B refers to calibrated radiance data at their original resolution with geolocation data stored in a separate file. We found that estimates of lake ice metrics were within $\pm 10\%$ cover using the two products, so Rapidfire images formed the interpretation dataset for this research. We also investigated surface reflectance products for lake ice, but a lack of reference aerosol data over our study area resulted in uneven data quality and a large amount of missing data. For the longer term monitoring project, registered 250 m calibrated radiance data will be collected to create a full archive for the study area, and 25 lakes in the region will be monitored for lake ice metrics (Reed et al., 2006).

Percent ice cover was manually interpreted for the five large focus area lakes from daily MODIS Rapidfire natural-color images. These lakes range in size from 4700–29,700 ha (Table 1), far larger than a conservative minimum mapping unit of 100 ha. Seasonal lake ice metrics were calculated from the dates of ice cover: break-up date, freeze-up date and durations of ice season, break-up season, and freeze-up season.

Ice appears as white on natural-color images, so snow-covered ice is easily interpreted. Likewise, open water is predominantly black or dark blue on image composites, with lighter blue signifying sediment load from glacial silt or volcanic ash (Fig. 2). Wet ice, which may occur during break-up, by overflow, or from mid-winter rain on solid ice, appears pale blue. Wet ice is often mottled with white and black, reflecting the ice and water mosaic. Another form of blue ice occurs when the frozen-over lake is windswept during winter storms. Pressure cracks are often visible in the imagery, indicating ice rather than open, silty water.

Freeze-up date was defined to occur when ice cover was $>90\%$, break-up date was when ice cover was $<10\%$, and ice season duration was the number of days between freeze-up and break-up (Jeffries et al., in press). There were often small areas ($<10\%$) of open water at the lake outlets during freeze-up, or wind stacked ice pans on the windward shore during break-up. These limited areas of residual open water and/or ice were not included in estimates of ice season duration as they are not expected to have much ecological impact on the lake systems.

We attempted to use various digital analysis techniques (density slice, several classification approaches) on the georeferenced calibrated radiance data. However, spectral confusion with clouds and fog, topographic and cloud shadows, and ice fracture features like pressure ridges, pans and open leads all contributed to serious misclassification errors. Manual interpretation gave more accurate and faster results when compared with field observations (Table 2). We used density slices of clear-day calibrated radiance data to derive percent ice cover values for several dates with varying ice formation to evaluate the manual interpretations of individual interpreters. Visual interpretations were within $\pm 10\%$ of the digitally derived cover values.

2.2.3. Vegetation index

Vegetation phenology was derived from 250 m, 16-day NDVI data. The MODIS vegetation index product contains two vegetation indices: the normalized difference vegetation index (NDVI) and enhanced vegetation index (EVI) (Huete et al., 2002). These products are produced at three spatial resolutions (250 m, 500 m, and 1000 m) and at 16-day compositing intervals. Consistent with the other data used in this study, we used the highest resolution available — 250 m. The compositing process uses a constrained view-angle, maximum value approach, where the maximum vegetation index value over the 16-day period is retained, provided it meets a filtering requirement based on quality, cloud cover, and viewing geometry (van Leeuwen et al., 1999). Even though the constrained view-angle, maximum value composite method used to create the MODIS NDVI product is designed to reduce cloud cover and other types of atmospheric contamination, some spurious values persist that disturb the temporal profile of the vegetation signal, thus disrupting many phenology algorithms. Some of these disruptions are identified in the quality assurance data that are attached to each MODIS product and are masked out during a preprocessing step.

A smoothing procedure is then performed on the time series to eliminate the masked values (and persistent residual cloud contamination) that are in the data. There are many methods available for temporally smoothing the vegetation index signal, including the best index slope extraction (Viovy et al., 1992), compound mean and median filters (VanDijk et al., 1987), and splines (White et al., 1997). Bradley et al. (2007) use a two-step technique using a harmonic approach for modeling average annual phenology and a spline-based approach for modeling interannual phenology to eliminate drop-outs and data gaps. We used a weighted least-squares approach (Swets et al., 1999) that eliminates anomalous low vegetation index values and reduces time shifts caused by overgeneralization of the signal, which is an artifact of many smoothing techniques. The approach uses a moving temporal window to calculate a family of regression lines that is associated with each observation; the family of lines is then averaged at each point to provide a continuous temporal NDVI signal. Through experimentation with different smoothing parameters, such as window length and weighting values, temporal nuances in the time series are retained.

The derivation of phenologic metrics used in this study was based on the identification of critical points in the annual vegetation index curve that corresponded to start of season, end of season, and other phenologic events, on a pixel-by-pixel basis. Algorithms were created to identify these critical points based on statistical measures of the rate of change in values or the slope of the temporal NDVI curve. Methods for deriving phenology metrics include establishing a vegetation index threshold value at which various seasonal vegetation events take place (Lloyd, 1990) or using one of various curve-derived measures such as inflection points (Badhwar, 1982; Moulin et al., 1997), maximum curvature (Zhang et al., 2003), time of maximum increase (Jönsson & Eklundh, 2002), or delayed moving average (Reed et al., 1994). Reed et al. (2003) reviewed these and other methodological approaches and concluded that they may each be estimating

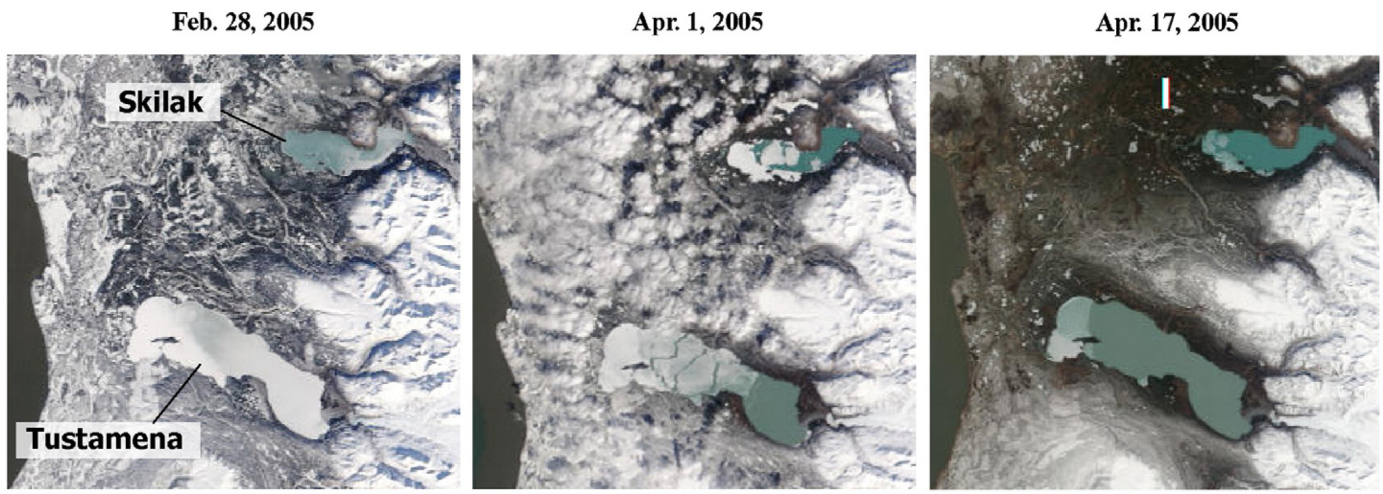

Fig. 2. Spring 2005 break-up of Skilak and Tustemena lakes. The Feb 28 image shows 100% ice cover on both lakes. Skilak (upper right corner of image) is predominantly bare ice, while Tustemena is mostly snow covered. By April 1 the ice pack on both lakes is largely fractured into loose pans. By April 17, only remnants of the ice cover persist at the western ends of the lakes.

fundamentally different phenologic phenomena, such as progressive stages of the vegetation's spring greenup (e.g., first sustained flush of greenness, primary leaf expansion, and early-season growth peak). The delayed moving average method established by Reed et al. (1994) was used for this work. Although the composite period was 16-days, the smoothing process resulted in data that could be interpolated to essentially a continuous temporal curve, thereby allowing the phenology metrics to be calculated with a daily time-step.

2.3. Comparison of derived metrics

We ran simple linear regressions in SAS (SAS Institute, Cary, NC) to examine relationships across years (2001–2007) between the onset of snowpack (snow on date) and the end of the growing season (end of season date); the end of snowmelt (snow off date) and the start of the growing season (start of season date); the onset of snowpack and the start of lake freeze-up (ice on date); and the end of snowmelt and the end of lake ice break-up (ice off date). We analyzed National Climatic Data Center mean daily temperature data from weather stations in the Cook Inlet Basin (Kenai, AK), Lime Hills (Pt. Alsworth, AK), and Alaska Peninsula (King Salmon, AK) focus areas to derive the number of days between November 1 and April 30 in each year that had a mean daily temperature of >0 °C (NCDC, 2008). We also compared graphical depictions of snow and ice depletion curves and growing season phenology to look for synchrony among the metrics (Fig. 3).

3. Results

3.1. Snow extent

The snow cover data showed greater temporal variability in start of season (snow on) than end of season (snow off) dates (Table 3). Interannual variability in the snow off date was lowest in the Alaska Peninsula and Lime Hills focus areas, whereas the Cook Inlet Basin area showed slightly more variability. In the case of the Alaska Peninsula, the snow off date varied by only 8 days throughout the 6-year series (Table 3). The snow season duration metric showed interannual consistencies within a focus area but greater variability among areas. Even though the Cook Inlet Basin had more variable snow on and snow off dates, it maintained a fairly consistent snow season duration with a difference of 24 days over the study period. This same consistency held true for the Alaska Peninsula, but the Lime Hills showed a more variable snow season duration with a difference of 56 days (Table 3).

Each focus area exhibited interannual variability in the timing and magnitude of snow-covered area, as illustrated by differences in the same 8-day composite period between 2005 and 2006 (Fig. 4). The Alaska Peninsula showed fairly consistent spatial patterns and magnitude of snow-covered area between years, while the Cook Inlet Basin showed more dramatic differences. In the case of the Lime Hills, both years met the snow on of 20% coverage. However, there

Table 2
Lake ice metrics for three focus areas in southwest Alaska.

	2001–02	2002–03	2003–04	2004–05	2005–06	2006–07
Cook Inlet Basin						
Skilak						
Ice on	12/7/01	–	1/2/04	1/18/05	1/17/06	1/5/07
Ice off	5/16/02	–	5/3/04	4/25/05	4/30/06	5/8/07
Ice duration	124	0	108	44	99	99
Tustamena						
Ice on	12/7/01	–	1/16/04	2/11/05	1/24/06	2/26/07
Ice off	5/16/02	–	5/3/04	5/2/05	4/30/06	5/3/07
Ice duration	146	0	94	33	94	49
Kenai (d MT>0 °C)	26	80	54	59	50	40
Lime Hills						
Telaquana						
Ice on	11/16/01	12/29/02	12/19/03	12/24/04	11/25/05	11/23/06
Ice off	6/3/02	5/13/03	5/22/04	5/14/05	6/1/06	5/22/07
Ice duration	178	125	153	134	185	161
Observed ice on	11/25/01	12/29/02		12/24/04	11/25/05	11/23/06
Observed ice off	5/25/02	5/9/03			5/30/06	5/22/07
Pt. Alsworth (d MT>0 °C)	54	109	61	81	49	50
Alaska Peninsula						
Kukaklek						
Ice on	12/4/01	12/31/02	12/26/03	12/25/04	12/27/05	12/5/06
Ice off	6/1/02	5/3/03	5/22/04	5/15/05	6/7/06	6/1/07
Ice duration	167	42	146	135	155	169
Nonvianuk						
Ice on	12/2/01	12/31/02	12/25/03	12/25/04	11/25/05	11/20/06
Ice off	5/25/02	4/29/03	5/20/04	5/15/05	6/3/06	5/27/07
Ice duration	167	51	128	120	178	181
King Salmon (d MT>0 °C)	50	98	58	27	35	46

Timing metrics are expressed as calendar date and duration metrics are number of days. A dash (–) indicates years without 100% ice cover. The temperature data is expressed as the number of days with mean temperatures greater than 0 °C (d MT>0 °C).

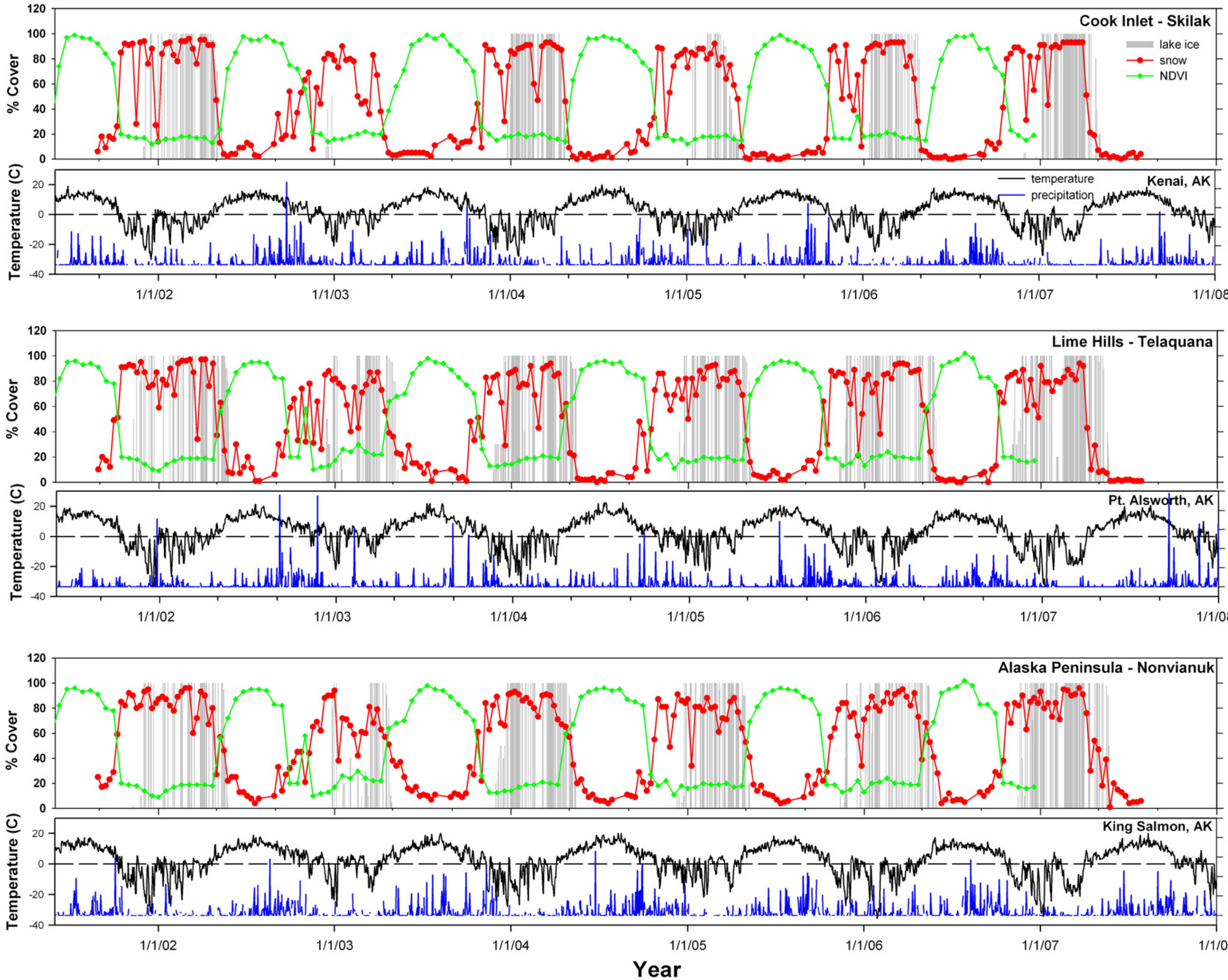

Fig. 3. Lake ice, snow, and vegetation metrics for the Cook Inlet Basin, Lime Hills, and Alaska Peninsula focus areas. Corresponding daily precipitation totals and mean daily temperatures recorded at Kenai, AK; Pt. Alsworth, AK; and King Salmon, AK are shown for each focus area. The strong El Niño of 2002–2003 resulted in reduced snow cover and a shortened lake ice season for all focus areas.

Table 3
Snow cover metrics for three focus areas in southwest Alaska.

	2001–02	2002–03	2003–04	2004–05	2005–06	2006–07
Cook Inlet Basin						
Snow on	10/08/01	09/22/02	10/16/03	09/22/04	10/24/05	10/16/06
Snow off	05/09/02	04/15/03	05/01/04	04/23/05	05/09/06	04/23/07
Snow duration	224	216	208	224	208	200
Lime Hills						
Snow on	09/30/01	09/06/02	10/08/03	09/22/04	10/08/05	10/08/06
Snow off	05/25/02	05/25/03	05/17/04	05/09/05	05/25/06	05/01/07
Snow duration	248	272	232	240	240	216
Alaska Peninsula						
Snow on	10/08/01	09/30/02	10/08/03	10/24/04	10/08/05	09/30/06
Snow off	05/25/02	05/25/03	06/02/04	06/02/05	06/02/06	06/02/07
Snow duration	240	248	248	232	248	256

Timing metrics are expressed as calendar date and duration metrics are number of days.

Table 4
Median vegetation phenology values by focus area.

	2001	2002	2003	2004	2005	2006
Cook Inlet Basin						
Start of growing season	04/23	05/03	04/24	04/16	04/21	04/27
End of growing season	10/30	11/14	11/03	10/26	10/20	11/06
Duration of growing season	190	185	196	191	185	193
Total NDVI	52	44	47	47	48	51
Lime Hills						
Start of growing season	05/17	05/08	05/01	04/25	05/03	05/10
End of growing season	10/22	10/25	10/27	10/17	10/18	10/26
Duration of growing season	156	170	174	178	169	168
Total NDVI	52	44	47	47	49	51
Alaska Peninsula						
Start of growing season	05/25	05/13	05/05	05/07	05/06	05/16
End of growing season	10/26	11/08	10/31	10/24	10/25	11/05
Duration of growing season	153	168	172	173	172	170
Total NDVI	51	45	49	47	49	52

Duration of growing season is recorded in days.

were significant differences in magnitude between the 2005 and 2006 images, with areal extents of 31% and 63% snow cover, respectively (Fig. 4).

3.2. Lake ice

Within the five focus lakes, freeze-up dates were more variable (~4–12 weeks) than break-up dates (~2–5 weeks) (Table 2). Actual start of freeze-up (>10% ice cover) was consistent across the region every year. Some higher elevation lakes in the Lime Hills and Alaska Peninsula focus areas (e.g., Nonvianuk and Kukaklek) froze early in the season and remained frozen until late in the spring, when they broke up very rapidly. For these lakes, break-up dates were consistent across years. Break-up dates on other lakes were much more variable, and in some years the lakes did not freeze at all (e.g., Skilak and Tustamena in 2002–03). Field observations collected by year-round residents on Telaquana Lake and image interpreted ice on and ice off dates differed by 8–10 days during 2001–03, and 0–3 days for 2004–07 (Table 2).

3.3. Vegetation phenology

The phenology data showed a range of median start of season dates of 13 days in the Cook Inlet Basin (21 April to 3 May), 20 days in the Alaska Peninsula (5 May to 25 May) and 22 days in the Lime Hills (25 April to 17 May) (Table 4). The median end of season metric varied from 20 October to 14 November in the Cook Inlet Basin (25 days), 17 to 27 October in the Lime Hills (10 days), and 24 October to 8 November in the Alaska Peninsula (15 days) (Table 4). Even with the wide ranging end of season dates for Cook Inlet Basin, the median length of growing season varied only by 11 days (185 to 196 days) over the six years. Both the Lime Hills and Alaska Peninsula focus areas showed a range of median end of season dates of around 3 weeks (156 to 178 days for Lime Hills and 153 to 173 days for Alaska Peninsula). The range of median total NDVI values for the three focus areas were very similar: 44 to 52 for Cook Inlet, 44 to 52 for Lime Hills, and 45 to 52 for Alaska Peninsula.

3.4. Relationships between metrics

Fig. 3 shows the time series (2001–2007) of all seasonal metrics that we are recording, along with daily temperature and precipitation, plotted for the three focus areas. We found that the start of the growing season and the timing of lake ice break-up coincided with snowmelt, but that snowpack formation in the fall had little effect on the timing of lake ice formation or growing season length. The timing of snowmelt appeared to coincide with both the start of the growing

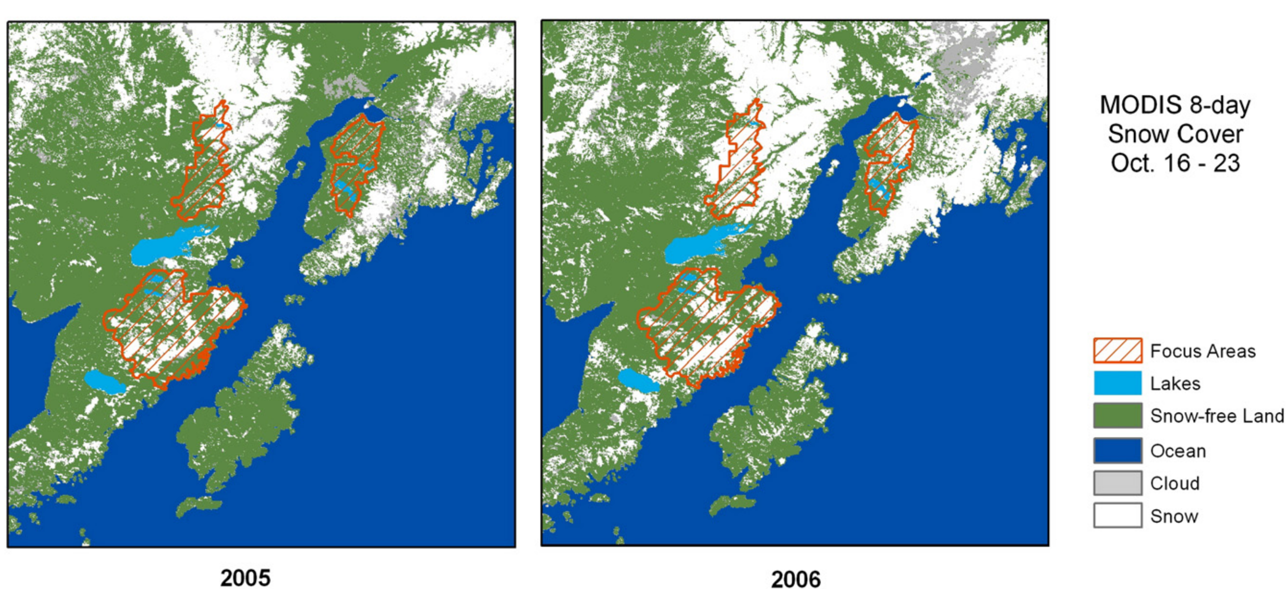

Fig. 4. A comparison of variability in snow cover extent during the middle of October for 2 years of the time series. Based on the start-of-season criteria previously described, the 2005–06 season has yet to start in the Cook Inlet Basin focus area, while the season is under way for the same area in the 2006–07 season.

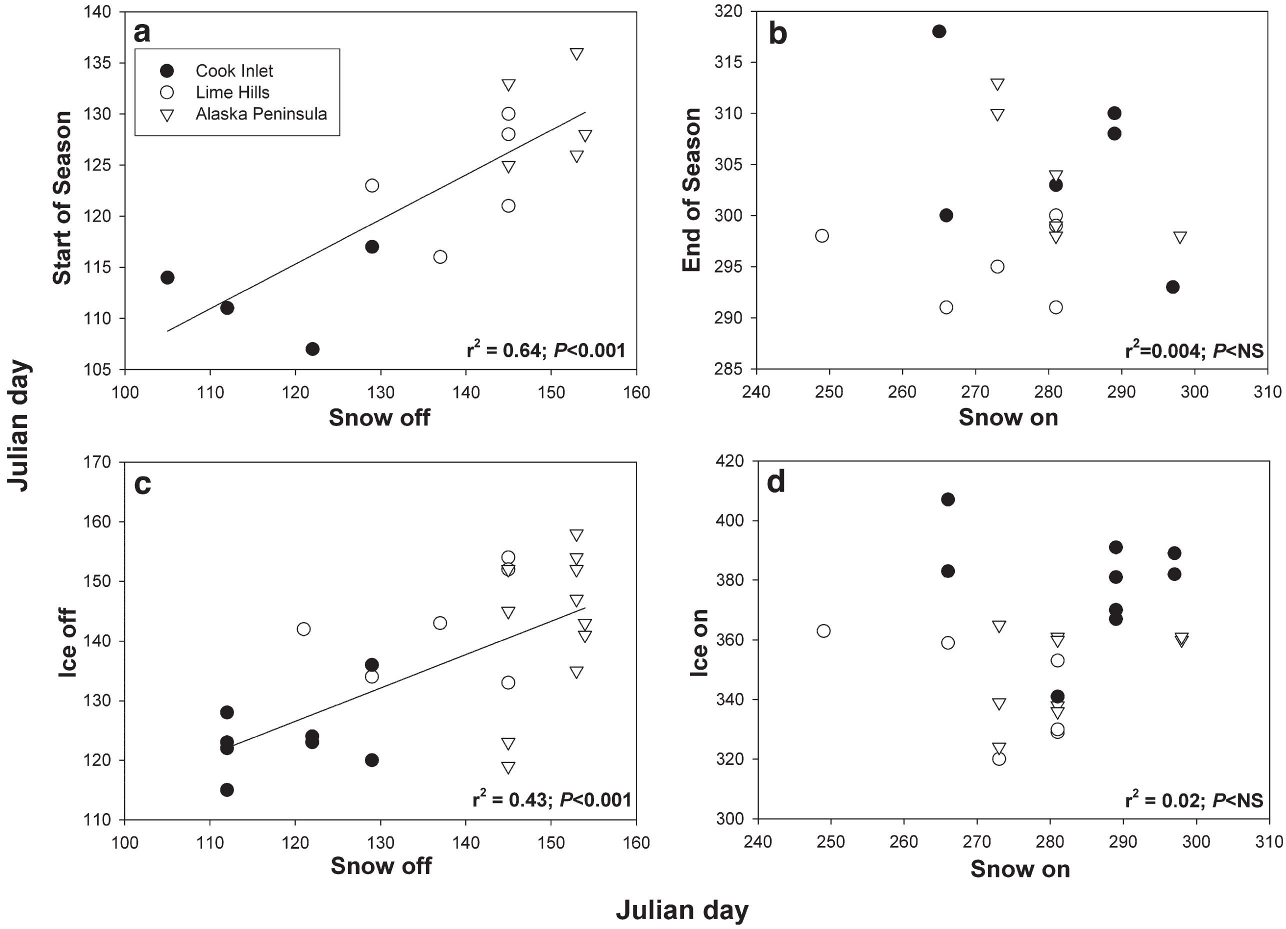

Fig. 5. Regressions of snow season (end of season, start of season) against growing season and lake ice season dates, by ecoregion-year. Lake ice dates are for Skilak and Tustamena (Cook Inlet); Telaquana (Lime Hills); and Kukaklek and Nonvianuk (Alaska Peninsula). (a) Snowmelt (snow off) versus start of growing season; (b) snowpack formation (snow on) versus end of growing season; (c) snowmelt versus lake ice break-up date (ice cover <10%); (d) snowpack formation versus lake freeze-up date (ice cover >90%).

season and the end of the lake ice season. The start of the growing season generally initiated at the end of the snow season, indicating that the initial flush of vegetative greenness occurred simultaneously with snowmelt as surface soil temperatures increased slightly above freezing (Fig. 3). We found a positive relationship between the timing of snowmelt (snow off) and time of the onset of growing season when the data were summarized over the three focus areas (Fig. 5a; $r^2=0.64$; $P<0.001$). Both the greening of vegetation and the loss of snow (e.g., through snowmelt) can contribute to an increase in the NDVI value, making separation of the two variables difficult. The high reflectance of snow-covered ground causes the NDVI to be lower than under snow-free conditions, and therefore melting snow is at least partially responsible for greening conditions (Dye & Tucker, 2003). However, because melting snow is associated with warming conditions that are capable of supporting photosynthesis, the two processes (melting snow and start of growing season) are logically associated with one another, especially in evergreen vegetation, which is common in the study area.

In the lowlands of the Cook Inlet Basin, the growing season generally didn't start until snow cover was 20% or less. In the more mountainous Lime Hills and Alaska Peninsula, NDVI began to increase when snow cover declined to approximately 50% (Fig. 3). The end of snow cover and start of growing season are both gradual processes and are highly temperature dependent in this environment. The timing of snow off (using a threshold of 20–30% snow cover) was typically one to two weeks after the median start of season for an ecoregion, as greening began before the snow was entirely gone from a region.

In contrast, there was no relationship between the timing of first snowfall (snow on) and the end of the growing season (Figs. 3 and 5b). The end of the growing season is also a gradual process that is both temperature and day-length dependent. The onset of snow cover, on the other hand, is an abrupt event that is not solely dependent on temperature. Likewise, we found no relationship between the timing of lake freeze-up (ice >90% cover) and snowpack formation (Fig. 5d), although lake ice formation consistently lagged the start of snow season by 2 to 3 months (Fig. 3).

As with the relationship between snow and NDVI, the end of snow season and final lake ice break-up dates were generally synchronous (Fig. 5c; $r^2=0.43$; $P<0.001$). Once mean ambient temperatures rose above 0 °C in the spring, lower elevation lakes in the Cook Inlet Basin focus area (e.g., Skilak and Tustamena) tended to break up within a period of several weeks. Higher elevation, interior lakes in the Lime Hills and Alaska Peninsula focus areas tended to show a greater lag in break-up. Weather records for 2001–2007 show that approximately 15 to 45% (Kenai), 30 to 60% (Pt. Alsworth), and 20 to 55% (King Salmon) of mean daily temperatures between November 1 and April 30 were above 0 °C (Table 2). El Niño years showed a two- to three-fold increase in the proportion of winter days above 0 °C, relative to neutral years.

4. Discussion

Preliminary interpretations of the MODIS data suggest that landscape-scale phenomena across the SWAN are complex. High variability in the timing of freeze-up, break-up, and duration of lake ice appeared to be related to variability in winter temperatures suggesting that winter conditions exert a strong influence on all of the metrics measured here. We found a general gradient of variability in the seasonality of the metrics: lake ice was the most variable, followed by snow metrics and vegetation metrics.

4.1. Effect of winter conditions on snow and lake ice season

The multiple factors driving the climate in southwest Alaska result in extremely variable temperatures, variation in the form and timing of precipitation, and in the location and strength of winter storms that ultimately control snow season and lake ice through their effect on freezing levels, wind patterns, and periods of freezing temperatures. These storms also affect vegetation metrics through the rate of warming (spring) and cooling (fall).

The period of record reported here has seen alternating El Niño and neutral winters, with a strong El Niño in 2002–03, a normal El Niño in 2004–05 and a weak El Niño in 2006–07 (Papineau, personal communication). Strong El Niños typically result in many warm temperature anomalies in southern Alaska (Papineau, 2001). The focus lakes tended to have shorter duration of ice season during El Niños, with the shortest seasons during the 2002–03 winter, and increasing ice duration in weakening El Niño winters of 2004–05 and 2006–07. Snow season, however, showed longer duration snow cover in the El Niño winters. This may have been caused by heavy precipitation in the fall at higher elevations. The timing and position of late fall storm tracks that bring colder temperatures and snow to the region could be a major contributor to the ice and snowpack characteristics for the entire winter. We expect that relatively small changes in temperature could have regional effects on snowpack and lake ice as winter temperatures fluctuate around 0 °C. The 2002–03 El Niño winter brought temperatures above 0 °C at elevations below 300 m. The result was rain at lower elevations and a diminished, thin snowpack, while a deep snowpack developed at higher elevations.

4.2. Variability in snow, lake ice, and growing season metrics

Over the period of this study (2001–2007), lake ice season (freeze-up and break-up dates; ice duration) showed high interannual variability, whereas snow and growing season metrics were more stable across years. Much of the vegetation in the focus areas consists of woody perennials rather than herbaceous annuals. Succession of plant communities is relatively slow, on the order of decades or longer, so vegetation metrics, as influenced by changes in vegetation cover (e.g., Sturm et al., 2005; Myneni et al., 1997) are expected to remain relatively stable over the duration of this project. However, increased variability in start- and end-of-season dates is likely with increasing variability in temperatures forecast for the 21st century (Crowley, 2000). Using 17 years of 8 km AVHRR NDVI data collected from 1982 to 1998, Hicke et al. (2002) showed changes in net primary productivity (based on NDVI) in Alaska and western Canada occurring in late spring and early summer, apparently associated with warmer early season temperatures. Likewise, earlier start-of-season and/or later end-of-season dates derived from 1989 to 2003 8 km AVHRR data appear to have contributed to increased growing season length in the Bristol Bay Lowlands and Kuskowim Delta, Alaska (Reed, 2006). As we build the higher resolution (250 m) MODIS database, we will be able to conduct similar analyses, but at a higher level of detail that is more suited to resource management.

Start of season and, indeed, any phenological metric estimated from satellite data, is extremely difficult to validate. It is even more difficult in an isolated area such as the SWAN where there is very little information to compare against. It is not entirely clear what start of season refers to at a 250 m pixel scale — whether it is when photosynthesis first begins, when the first sustained flush of greenness occurs, or when primary leaf expansion takes place (Reed et al., 2003). During a flight transect from Anchorage to Homer in early May 2004, we sought to verify where start of season was occurring by ocular estimate. Although our satellite derived data were later to show the median start of season in Cook Inlet Basin occurring on 16 April, we did not identify much green cover from the airplane except from evergreen coniferous trees. However, we did identify multiple instances of bear and moose grazing on early growing sedges, indicating that green vegetation was present (and likely detectable from satellite) that we could not see.

In contrast to vegetation metrics, lake ice is highly responsive to short-term weather events, developing overflow and partial ice breakup during windy Chinook storms and freezing overnight when a high pressure system moves into the area bringing cold temperatures and little wind. Snow cover was found to be moderately variable at the beginning of the snow season, whereas duration of snow cover and the end of season (snow off) dates were relatively consistent. Generally, a cold weather system brings snow that remains for weeks to months until warmer air masses move into the region. The timing of these cold weather systems is likely to remain erratic given the speculation for increasing temperature variability. Such variability in thermal regimes could potentially impact the duration of the snow season and the timing of snow cover depletion. The impacts of such changes could be far reaching.

Lake ice and snow cover are partial controls on many biological processes, including the growing season metrics reported here, as well as wildlife habitats and movements (Adams et al., 1995; Modafferi & Becker, 1997), salmon migrations and waterfowl nesting (Madsen et al., 2007). For example, the 2002–2003 El Niño winter led to a lack of insulating cover for vegetation at low elevations, wind desiccation, and frost damage (P. Spencer, unpublished data). Lack of snow cover limits subnivean travel of microtenes, an important set of prey species, exposing them to increased predation and cold stress (Courtin et al., 1991). Low or no snowpack enables large ungulates such as moose, caribou, and Dall sheep to access a wider range of sparse winter forage, but also allows wolves to travel more efficiently while hunting. Solid ice cover on lakes facilitates human travel for subsistence activities such as ice fishing, hunting, trapping, and wood cutting. Years with poor ice cover yield limited harvests and, often, accidents involving travelers going through the ice. An early start of season, as was observed in the spring of 2004 in the Cook Inlet Basin, means that protein-rich sedges are available to nursing bear sows and pregnant moose during a stressful and vulnerable time of their lives.

5. Summary and conclusions

A set of ecologically oriented metrics was derived from a series of MODIS products to assess interannual variability in snowpack, lake ice, and vegetation dynamics in southwest Alaska. The lake ice and snow metrics reported here appeared to be strongly influenced by global and regional climate and local topography, and represent the dynamics of the physical processes on the SWAN landscape.

Lake ice showed the greatest temporal variation of the observed seasonal metrics, followed by snow cover and then vegetation metrics. This pattern is likely due to the factors controlling ice, snow and vegetation. The derivation and analysis of separate but related sets of satellite-generated, ecologically meaningful metrics gives us the opportunity to examine ecosystem function at a scale that has not been previously tenable. For long-term monitoring, we need simple analysis techniques and easily interpreted metrics that are neither sensor nor format specific. However, we do need sensor packages that are of moderate spatial resolution and high temporal resolution with visible, near-infrared, and mid-infrared wavelengths. Continuity of such sensor systems is critical to long-term ecological monitoring.

The data provide an overview of ecosystem-wide seasonal dynamics that can be compared across years. The length of record currently imposes limitations on the types of conclusions that can be drawn, but the growing data archive has already provided evidence of potential linkages among snowpack, lake ice, and vegetation dynamics.

Acknowledgements

We acknowledge the contributions of Jeanette and Jerry Mills, National Park Service volunteers-in-residence at Telaquana Lake, for their meticulous records of lake ice cover and associated weather records for the last 7 years. Their data have served as a gratifying confirmation of the ice season interpretations and provided explanations for unusual ice phenomena. We appreciate John Papineau, NOAA, for patient discussions about climate patterns in SW Alaska. This project was funded by the National Park Service Inventory and Monitoring Program, Southwest Alaska Network.

References

Adams, L. G., Singer, F. J., & Dale, B. W. (1995). Caribou calf mortality in Denali National Park, Alaska. *Journal of Wildlife Management*, *59*, 584−594.

Badhwar, G. D. (1982). Crop emergence date determination from spectral data. *Photogrammetric Engineering and Remote Sensing*, *46*, 369−377.

Bradley, B. A., Jacob, R. W., Hermance, J. F., & Mustard, J. F. (2007). A curve-fitting technique to derive inter-annual phenologies from time series of noisy satellite data. *Remote Sensing of Environment*, *106*, 137−145.

Courtin, G. M., Kalliomaki, N. M., Hillis, T., & Robitaille, R. L. (1991). The effect of abiotic factors on the overwintering success in the meadow vole, *Microtus pennsylvanicus*: Winter redefined. *Arctic and Alpine Research*, *23*, 45−52.

Crowley, T. J. (2000). Causes of climate change over the past 1000 years. *Science*, *289* (5477), 270−277.

Davey, C. A., Redmond, K. T., & Simeral, D. B. (2007). Weather and climate inventory, National Park Service, Southwest Alaska Network. *Natural resource technical report NPS/SWAN/NRTR-2007/045* 80 pgs.

Delbart, N., Kergoat, L., Le Toan, T., Lhermitte, J., & Picard, G. (2005). Determination of phenological dates in boreal regions using normalized difference water index. *Remote Sensing of Environment*, *97*, 26−38.

Déry, S. J., Salomonson, V. V., Stieglitz, M., Hall, D. K., & Appel, I. (2005). An approach for using snow areal depletion curves inferred from MODIS and its application to land surface modeling in Alaska. *Hydrological Processes*, *19*, 2755−2774.

Dye, D. G., & Tucker, C. J. (2003). Seasonality and trends of snow-cover, vegetation index, and temperature in northern Eurasia. *Geophysical Research Letters*, *39*(7), 1405. doi:10.1029/2002GL016384

Fancy, S. G., Gross, J. E., & Carter, S. L. (2009). Monitoring the condition of natural resources in U. S. national parks. *Environmental Monitoring and Assessment*, *151*, 161−174.

Gaul, K. K. (2007). *NANUTSET ch'u Q'udi Gu, before our time and now. An ethnohistory of Lake Clark National Park and Preserve. USDOI, NPS, Lake Clark National Park and Preserve* 179 pgs.

Goetz, S. J., Bunn, A. G., Fiske, G. J., & Houghton, R. A. (2005). Satellite-observed photosynthetic trends across boreal North America associated with climate and fire disturbance. *Proceedings of the National Academy of Sciences of the United States of America*, *102*(38), 13521−13525.

Hall, D. K., & Riggs, G. A. (2007). Accuracy assessment of the MODIS snow products. *Hydrological Processes*, *21*(12), 1534−1547.

Hall, D. K., Riggs, G. A., & Salomonson, V. V. (1995). Development of methods for mapping global snow cover using Moderate Resolution Imaging Spectroradiometer (MODIS) data. *Remote Sensing of Environment*, *54*, 127−140.

Hicke, J. A., Asner, G. P., Randerson, J. T., Tucker, C., Los, S., Birdsey, R., et al. (2002). Trends in North American net primary productivity derived from satellite observations, 1982–1998. *Global Biogeochemical Cycles*, *16*(2), 1018. doi:10.1029/2001GB001550

Huete, A., Didan, K., Miura, T., Rodriguez, E., Gao, X., & Ferreira, L. (2002). Overview of the radiometric and biophysical performance of the MODIS vegetation indices. *Remote Sensing of Environment*, *83*, 195−213.

Jeffries, M. O., Morris, K., & Duguay, C. R. Lake ice and river ice. In R. S. Williams Jr. & J. G. Ferrigno (Eds.), *State of the Earth's cryosphere at the beginning of the 21st century: Glaciers, snow cover, floating ice, and permafrost and periglacial environments. Satellite image atlas of glaciers of the world, introduction and synthesis, Volume 1386-A, U.S.* Geological Survey, in press.

Jönsson, P., & Eklundh, L. (2002). Seasonality extraction by function fitting to time-series of satellite sensor data. *IEEE Transactions on Geoscience and Remote Sensing*, *40*(8), 1824−1832.

Justice, C. O., Vermote, E., Townshend, J. R. G., Defries, R., Roy, D. P., Hall, D. K., et al. (1997). The Moderate Resolution Imaging Spectroradiometer (MODIS): Land remote sensing for global change research. *IEEE Transactions on Geoscience and Remote Sensing*, *36*, 1228−1249.

Lammers, R. B., Shiklomanov, A. I., Vörösmarty, C. J., Fekete, B. M., & Peterson, B. J. (2001). Assessment of contemporary Arctic river runoff based on observational discharge records. *JGR-Atmospheres*, *106*(D4), 3321−3334.

Lloyd, D. (1990). A phenological classification of terrestrial vegetation cover using shortwave vegetation index imagery. *International Journal of Remote Sensing*, *11*, 2269−2279.

Madsen, J., Tamstorf, M., Klaassen, M., Eide, N., Glahder, C., Rigét, F., et al. (2007). Effects of snow cover on the timing and success of reproduction in high-Arctic pink-footed geese *Anser brachyrhynchus*. *Polar Biology*, *30*(11), 1363−1372.

Magnuson, J. J., Robertson, D. M., Benson, B. J., Wynne, R. H., Livingstone, D. M., Arai, T., et al. (2000). Historical trends in lake and river ice cover in the northern hemisphere. *Science*, *289*, 1743−1746.

Modafferi, R. D., & Becker, E. F. (1997). Survival of radiocollared adult moose in Lower Susitna River Valley, southcentral Alaska. *Journal of Wildlife Management*, *61*, 540−549.

Moulin, S., Kergoat, L., Viovy, N., & Dedieu, G. (1997). Global-scale assessment of vegetation phenology using NOAA/AVHRR satellite measurements. *Journal of Climate*, *10*, 1154−1170.

Myneni, R. B., Dong, J., Tucker, C. J., Kaufmann, R. K., Kauppi, P. E., Liski, J., et al. (2001). A large carbon sink in the woody biomass of northern forests. *Proceedings of the National Academy of Sciences of the United States of America*, *98*(26), 14784−14789.

Myneni, R. B., Keeling, C. D., Tucker, C. J., Asrar, G., & Nemani, R. R. (1997). Increased plant growth in the northern high latitudes from 1981–1991. *Nature*, *386*, 698−702.

Nowacki, G., Spencer, P., Fleming, M., Brock, T., and Jorgenson, T. (2002). Unified ecoregions of Alaska B2001. Digital data available: http://agdc.usgs.gov/data/projects/fhm/ USGS Open File Report 02-297. 1 map.

Papineau, J. M. (2001). Wintertime temperature anomalies in Alaska correlated with ENSO and PFO. *International Journal of Climatology*, *21*, 1577−1592.

Reed, B. C. (2006). Trend analysis of time-series phenology of North America derived from satellite data. *GIScience and Remote Sensing*, *43*, 24−38.

Reed, B. C., Brown, J. F., VanderZee, D., Loveland, T. L., Merchant, J. W., & Ohlen, D. O. (1994). Measuring phenological variability from satellite imagery. *Journal of Vegetation Science*, *5*, 703−714.

Reed, B. C., Budde, M., Spencer, P., & Miller, A. (2006). *Satellite-derived measures of landscape processes: Monitoring protocol for the Southwest Alaska I&M Network. National Park Service, Inventory & Monitoring Program, Southwest Alaska Network, Anchorage, Alaska* 30 pp.

Reed, B. C., White, M. A., & Brown, J. F. (2003). Remote sensing phenology. In M. D. Schwartz (Ed.), *Phenology: An integrative environmental science* (pp. 365−381). New York: Springer Publishing.

Simpson, J. J., Stuart, M. C., & Daley, C. (2007). A discriminate analysis model of Alaskan biomes based on spatial climatic and environmental data. *Arctic*, *60*, 341−369.

Sturm, M., Schimel, J., Michaelson, G., Welker, J. M., Oberbauer, S. F., Liston, G. E., et al. (2005). Winter biological processes could help convert arctic tundra to shrubland. *BioScience*, *55*, 17−26.

Swets, D. L., Reed, B. C., Rowland, J. D., & Marko, S. E. (1999). A weighted least-squares approach to temporal NDVI smoothing. *Proceedings of the 1999 ASPRS annual conference, from image to information, Portland, Oregon, May 17–21, 1999* Bethesda, Maryland: American Society for Photogrammetry and Remote Sensing [CD-ROM].

Townshend, J. R. G., & Justice, C. O. (2002). Towards operational monitoring of terrestrial systems by moderate resolution remote sensing. *Remote Sensing of Environment*, *83*, 351−359.

VanDijk, A., Callis, S. L., Sakamoto, C. M., & Decker, W. L. (1987). Smoothing vegetation index profiles: An alternative method for reducing radiometric disturbance in NOAA/AVHRR data. *Photogrammetric Engineering and Remote Sensing*, *53*, 1059−1067.

van Leeuwen, W. J. D., Huete, A. R., & Laing, T. W. (1999). MODIS vegetation index compositing approach: A prototype with AVHRR data. *Remote Sensing of Environment*, *69*, 264−280.

Viovy, N., Arino, O., & Belward, A. S. (1992). The best index slope extraction: A method for reducing noise in NDVI time series. *International Journal of Remote Sensing*, *13*, 1585−1590.

White, M. A., Thornton, P. E., & Running, S. W. (1997). A continental phenology model for monitoring vegetation responses to interannual climatic variability. *Global Biogeochemical Cycles*, *11*, 217−234.

Zhang, X. Y., Friedl, M. A., Schaaf, C. B., Strahler, A. H., Hodges, J. C. F., Gao, F., et al. (2003). Monitoring vegetation phenology using MODIS. *Remote Sensing of Environment*, *84*, 471−475.

Zhang, X., Harvey, K. D., Hogg, W. D., & Yuzyk, T. R. (2001). Trends in Canadian streamflow. *Water Resources Research*, *37*, 987−998.